Electroformation of Giant Unilamellar Vesicles on Stainless Steel Electrodes

Journal:	*ACS Omega*
Manuscript ID	ao-2016-00395k.R2
Manuscript Type:	Article
Date Submitted by the Author:	15-Feb-2017

Complete List of Authors:	Pereno, Valerio; University of Oxford Carugo, Dario; University of Southampton, Engineering Sciences Bau, Luca; University of Oxford Sezgin, Erdinc; University of Oxford, Bernardino de la Serna, Jorge; Science and Technology Facilities Council, Central Laser Facility Eggeling, Christian; University of Oxford , Weatherall Institute of Molecular Medicine Stride, Eleanor; University College London, Mechanical Engineering

Electroformation of giant unilamellar vesicles on stainless steel electrodes

Valerio Pereno[†], *Dario Carugo*[†,‡], *Luca Bau*[†], *Erdinc Sezgin*[§], *Jorge Bernardino de la Serna*[I], *Christian Eggeling*[§] *and Eleanor Stride**,[†]

[†]Institute of Biomedical Engineering, Department of Engineering Science, University of Oxford, Oxford, OX3 7DQ, United Kingdom

[‡]Mechatronics and Bioengineering Science research groups, Faculty of Engineering and the Environment, University of Southampton, SO17 1BJ, Southampton, United Kingdom

[§]Wetherall Institute of Molecular Medicine, Department of Immunology, University of Oxford, Oxford, OX3 9DS, United Kingdom

[I]Science and Technology Facilities Council, Rutherford Appleton Laboratory, Central Laser Facility, Research Complex at Harwell, Harwell-Oxford, OX11 0FA, United Kingdom

ABSTRACT

Giant unilamellar vesicles (GUVs) are well-established model systems for studying membrane structure and dynamics. Electroformation, also referred to as electro-swelling, is one of the most prevalent methods for producing GUVs, as it enables modulation of the lipid hydration process to form relatively mono-disperse, defect-free vesicles. Currently, however, it is expensive and time-consuming compared to other methods. In this study, we demonstrate that 1,2-dioleoyl-sn-glycero-3-phosphatidylcholine (DOPC) GUVs can be prepared readily at a fraction of the cost on stainless steel electrodes such as commercially available syringe needles, without any evidence of lipid oxidation or hydrolysis.

KEYWORDS

Electroformation; electroswelling; giant unilamellar vesicles; stainless steel electrode; platinum wire; generalized polarization; lipid packing; DOPC; lipid oxidation; lipid hydrolysis.

INTRODUCTION

Giant unilamellar vesicles (GUVs), often referred to as giant liposomes, are fluid-filled membranes that offer a useful basic model of a biological cell. GUVs have been widely used as models to study the fluid-fluid and gel-fluid phase coexistence of membrane lipids,[1–6] membrane transport phenomena,[7–12] the behaviour of native membranes,[13–16] the structure of early cells and protocells,[17] and more recently, cell biological activity.[10] In its simplest form a GUV consists of a single amphiphilic lipid bilayer that encloses an aqueous solution.

Among the multitude of production methods developed over several decades,[18–20] lipid film hydration,[21] electroformation,[22] lipid emulsification,[23,24] and microfluidic-based methods such as fluid jetting[25] and hydrodynamic flow focusing[26] are the most widely used. While the vesicle formation literature is rich with established formation protocols, each technique has its own inherent drawbacks and tradeoffs according to the application. The factors that affect the choice of a specific protocol include: technical expertise, the need for specialist equipment, and the degree to which vesicle characteristics need to be tuned. Of the methods cited above, electroformation is one of the most widespread.[18]

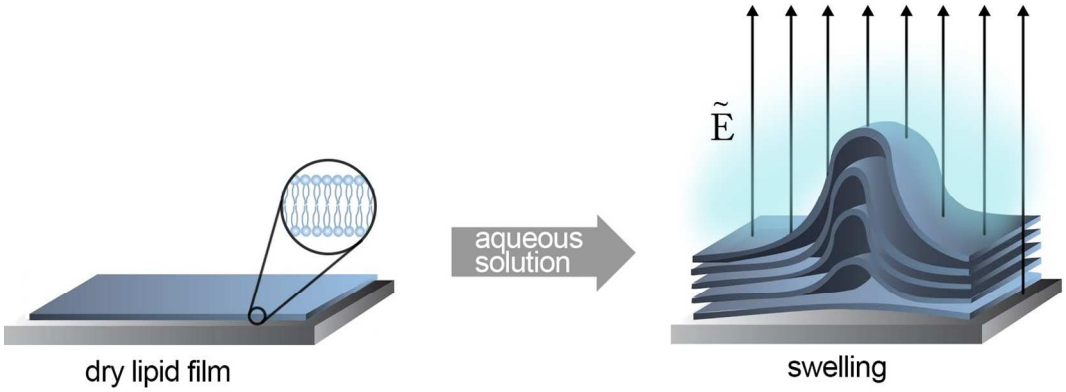

Figure 1. Schematic of vesicle electroformation from a dry lipid bilayer deposited on a substrate. Vesicles are formed upon hydration and application of an alternating electric field, $\tilde{E}$ (not to scale).

Electroformation of GUVs was pioneered by Angelova and Dimitrov in 1986[22]. It involves modulating the spontaneous swelling of lipids within an aqueous solution using an externally applied electric field. Typically, a solution of lipids dissolved in an organic solvent is deposited on two electrodes of indium tin oxide (ITO) coated glass or platinum. Following solvent evaporation, the electrodes are placed in contact with an aqueous solution. Subsequently, an alternating potential difference is applied across the electrodes, stimulating the swelling process of the hydrated lipid layer. The main advantages of electroformation are that it requires comparatively little technical expertise to implement and that it yields spherical, relatively monodisperse, and unilamellar lipid vesicles. Set against this, however, is the cost of the electrodes, which limit the scalability of the technique.

In this paper, we present and validate a simple electrode modification in the standard electroformation protocol that reduces cost and chamber preparation time while improving scalability. 1,2-dioleoyl-*sn*-glycero-3-phosphatidylcholine (DOPC) was chosen as a representative unsaturated phospholipid, which is more prone to oxidation than saturated phospholipids such as 1,2-distearoyl-*sn*-glycero-3-phosphocholine (DSPC), 1,2-dipalmitoyl-*sn*-glycero-3-phosphocholine (DPPC) and 1,2-dimyristoyl-*sn*-glycero-3-phosphocholine (DMPC), to prove that stainless steel does not affect its structural integrity.

Stainless steel electrodes such as an injection needles provide a significantly lower cost alternative to platinum and ITO electrodes, which are the established electrode materials reported in the electroformation literature. Other studies have also reported electroformation of vesicles on interdigitated and non-conductive substrates,[27] albeit with limited adoption rates.

Stainless steel electrodes provide numerous advantages. Firstly, the rigidity of stainless steel compared to platinum reduces the risk of bending, improving control over electrode separation

distance, thus leading to a more uniform electric field. In addition, disposable needles do not require cleaning in an ultrasound bath,[28] are readily available, and do not require the modification of current chambers.

The wide cost disparity between stainless steel and platinum enables two secondary modifications to the electroformation protocol: the use of longer electrodes and chamber parallelisation.[29] These lead, in turn, to an increase in overall vesicle production, concurrent electroformation and multi-parametric testing at high throughput.

While direct comparison between electroformation methods is complex, Table 1 provides an overview of the merits and drawbacks of different electrode materials used in the electroformation of vesicles. To populate the table, the electrode surface area was fixed across all methods. The cost comparison was carried out on the face-value of the electrodes, without taking into account the cost of the purpose-built, polyoxymethylene electroformation chamber. A full cost breakdown of the electroformation chamber is provided in the Supporting Information (Table S1). It is worthy of note that, if the stainless steel electrodes were disposed of after every electroformation experiment, it would take approximately 292 experiments to match the cost of the platinum electrodes – ignoring overheads such as the time and cost of cleaning.

In the experiments reported here, these features are exploited using a purpose-built electroformation device, which consists of a polyoxymethylene base containing five electroformation chambers and a lid to hold the electrodes in position.

Table 1. Summary of costs, advantages, and disadvantages of using stainless steel electrodes compared to platinum during electroformation. A detailed cost breakdown of the electroformation chamber is provided in the Supporting Information. [a] Calculated for five pairs of 40 mm cylindrical electrodes with a diameter of 0.8 mm or an ITO surface of equivalent area (10 cm^2).

	Cost[a]	Disposable	Scalable	Machinable	Cleaning required	Consistent electrode separation
Platinum	~£584	Expensive	Expensive	Yes	Yes	Difficult
Stainless steel	~£2.00	Yes	Yes	Yes	Only if reused	Yes
ITO coated glass	~£27.00	Yes	Yes	No	Yes	Yes

To validate the proposed technique, vesicles were characterised in terms of their size distribution, lipid packing, and unilamellarity of the vesicles' membrane. In addition, the aqueous electroformation solution constituents were analysed using inductively coupled plasma optical emission spectroscopy (ICP-OES) to test whether any ions are released from the electrodes during electroformation. Lipid degradation was assessed by nuclear magnetic resonance (NMR).

RESULTS AND DISCUSSION

Giant unilamellar vesicles production and imaging

Electroformation visualisation chambers have been used to monitor and verify the effective production of vesicles.[30] To assess the vesicle formation on stainless steel electrodes, swelling was visualised *in situ* (Figure 3a) using a second specially designed electroformation chamber with optical access using the protocol described in the Methods section. Vesicle formation was observed across most of the electrode surface, even prior to the application of the electric field (Figure 3a). Upon switching on the signal generator, the swelling was accelerated and vesicles reached moderate size (see supplementary video). DOPC vesicles swelling and detaching from an electrode were also observed (Figure 3b and 3c).

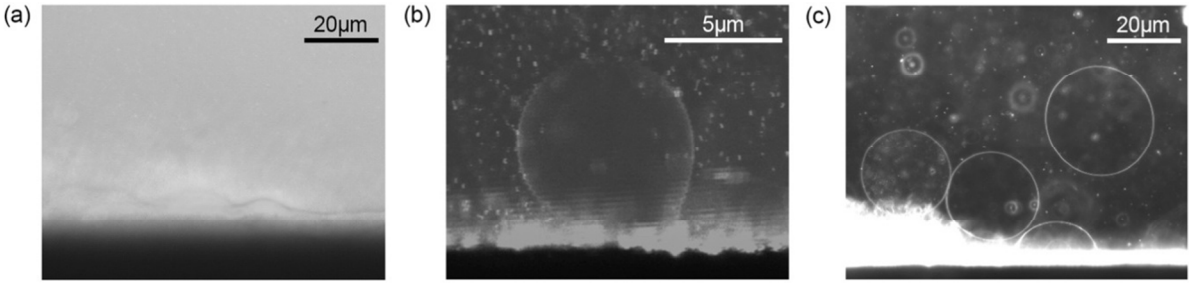

Figure 2. Vesicles swelling from electroformation electrodes: (a) hydrated lipid later commencing the swelling process, (b) DiI labelled single vesicle swelling while attached to the electroformation electrodes and (c) vesicles forming, swelling and detaching along the electrode.

Following the visualisation, vesicles were produced inside the device depicted in Figure 2a using the electroformation protocol described in the Materials and methods section. The electrode material did not produce significant differences in the size distributions of the vesicles (Figure 4) and were within the ranges reported in existing literature (10-30 μm for DOPC vesicles)[27,31,32]

The yield of a single electroformation chamber was estimated by suspending 100 μL of GUV-rich solution in PBS and counting the number of vesicles at the bottom of a visualisation plate after allowing the vesicles to sediment. The vesicles were counted using a purpose-built algorithm for both electrode materials. On average, the stainless steel electrode electroformation yielded 2256 vesicles (22560 vesicles/mL), against the 3114 (31140 vesicles/mL) yielded by the platinum wire electrodes. The difference however was not statistically significant.

It should be noted, however, that comparison between GUV studies is problematic due to differences in experimental parameters such as differences in osmotic pressure, electrode size and separation, electroformation solution, lipid specie, electric field strength, focal plane, and vesicle manipulation technique.

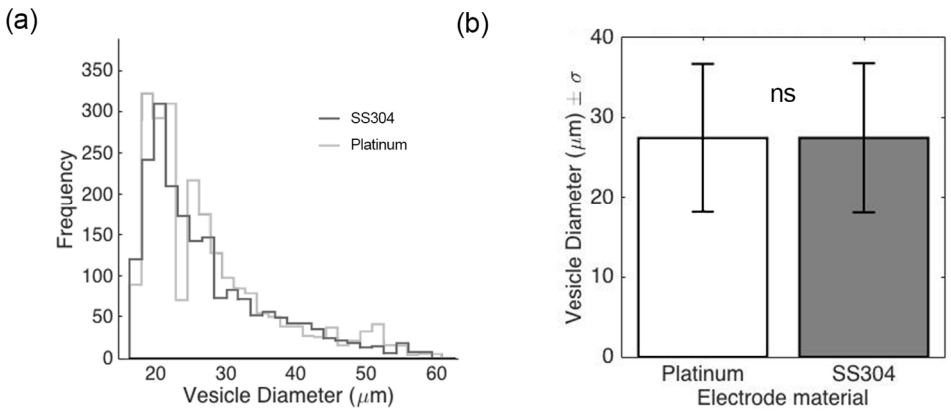

Figure 3. (a) DOPC vesicle size distribution as a function of electrode material. The white bars represent vesicles formed using platinum wires as electrodes, while the grey bars represent vesicles formed using stainless steel electrodes. (b) Average vesicle diameter (± standard deviation) comparison for platinum and stainless steel electrodes. Three independent experiments were conducted and over 1500 vesicles were analysed for each electrode material.

Lipid order and size of vesicles composed of binary lipid mixtures

To test the parallelisation potential, vesicles with different compositions were produced simultaneously by varying the DOPC:cholesterol (DOPC:Chol) molar ratio in the multi chamber device.

The results depicted in Figure 5 were obtained by performing four concurrent electroformation experiments, coating the wires in each chamber with a different lipid composition. Figure 5a displays the average GPs and standard deviations of the vesicles for each initial lipid composition. As the cholesterol volume fraction increases, the packing of the membrane also increases, as cholesterol intercalates between the DOPC lipids.[33–35] The electroformation cycle lasted for 2.5 hrs, required limited set-up time, and was performed using 4 pairs of new injection needles (SS304), at a total electrode cost of approximately £2.00. The equivalent cost of Pt wire

electrodes would have been approximately £584 and would have required electrode cleaning and straightening.

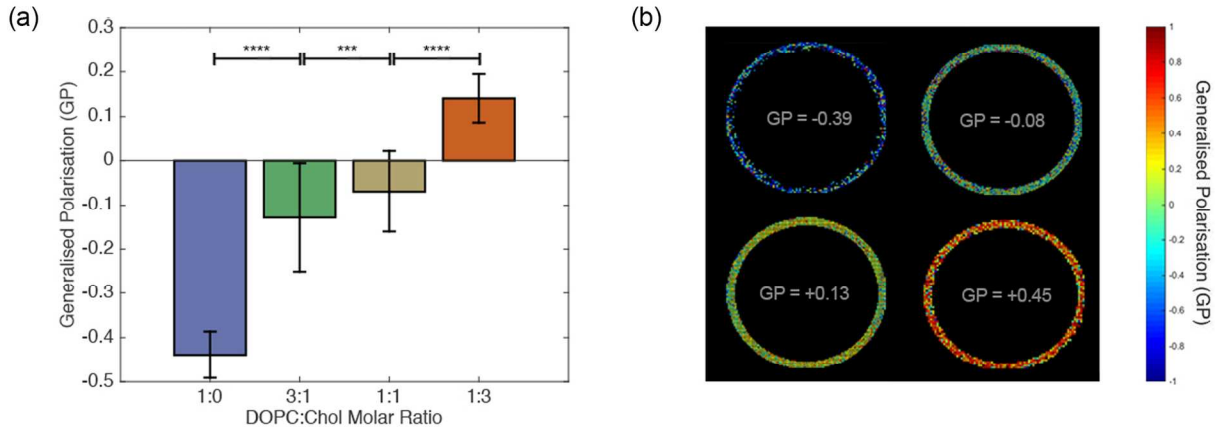

Figure 4. Simultaneous electroformation of vesicles with dissimilar membrane properties: (a) Generalised Polarisation of the vesicles as a function of initial lipid film formulation; (b) Representative GP false-coloured images of four vesicles with different GP values.

The consistency in vesicle diameter was determined as a function of lipid composition. The vesicle size was not affected significantly by the molar fraction of cholesterol when compared to the 1:0 DOPC:Chol composition (Figure 6a). The electrode material did not have an effect on the lipid packing of GUV electrodes (Figure 6b). A higher osmolarity of the extravesicular environment yields vesicles with a higher membrane order, and thus a higher degree of lipid packing.[36]

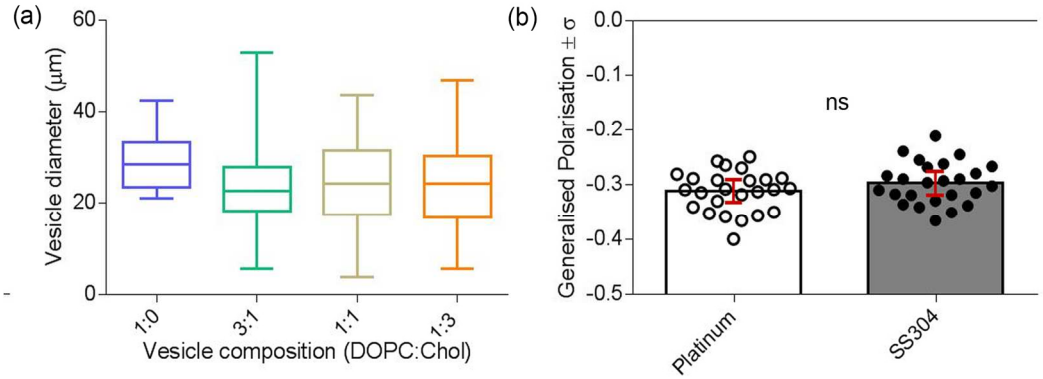

Figure 5. Simultaneous electroformation of vesicles with dissimilar membrane properties: (a) Generalised Polarisation of the vesicles as a function of initial lipid film formulation; (b) Representative GP false-coloured images of four vesicles with different GP values.

Leaching of metals from the electrodes

Leaching of transition metals from the electrodes can be a concern in electroformation of GUVs. Metal ions can bind to membranes[37] and alter their bilayer structure,[38] phase behavior[39] and stability against vesicle fusion.[40] Unwanted chemical reactions can also be catalyzed by trace metals: chromium, iron and nickel can initiate, and in some cases propagate, lipid peroxidation.[41]

The possibility of leaching of metals from the stainless steel electrodes under electroformation conditions was assessed by comparing the concentration of its constituents (Fe, Cr, Ni, and Mn) in GUV samples (Table 2) prepared with stainless steel electrodes and platinum electrodes. No increase in metal concentration compared to platinum electrodes was detected by inductively coupled plasma optical emission spectroscopy (ICP-OES). While no evidence of ion leaching was detected when the electroformation was carried out in 200 mM sucrose, this may not be the case in conductive electroformation solutions. On the contrary, platinum electrodes are routinely used to electroform vesicles in solutions of physiological ionic strength. A similar argument holds true for temperature, as electroformation of vesicles with higher transition temperatures require a heated chamber.

Table 2. Concentrations of alloy constituents inside the electroformation chamber. The concentrations for both platinum and stainless steel electrodes are shown.

Element	% fraction in SS304	Concentration with Pt electrodes (ppm)	Concentration with SS304 electrodes (ppm)
Iron	65-71	<0.1	<0.1
Chromium	18-20	<0.1	<0.1
Nickel	8-12	<0.1	<0.1
Manganese	2	<0.1	<0.1

Lipid oxidation and hydrolysis

Products of lipid oxidation and hydrolysis, which can be generated at the electrode during the electroformation process,[42] are also known to affect the physical properties of phospholipid membranes. Even small amounts of degradation products can cause structural and dynamic changes, such as the formation of lipid rafts[42] or changes in permeability[43] and mechanical stability.[44] ^{1}H-NMR and ^{31}P-NMR spectroscopy are among the fastest and most informative analytical methods that have been used to characterize the chemical structure of phospholipids extracted from biological membranes and their degradation products.[45–48] The structural integrity of electroformed GUVs was assessed by comparing NMR spectra of the combined lipid extracts from nine electroformed GUV samples with a control obtained from large multilamellar vesicles (LMVs) prepared by lipid hydration. The ^{1}H-NMR spectra of lipids extracted from electroformed GUVs and from LMVs are compared in Figure 6. The spectra are identical, and both are consistent with pure DOPC. No degradation products were detected within a limit of detection of 1 mol%. Although trace impurities can be seen in the electroformed sample, the same impurities are found in the control. Their concentration remains constant as the concentration of DOPC in the control sample is increased from 0.34 mM to 3.4 mM, suggesting that they could be due to trace contamination rather than lipid degradation.

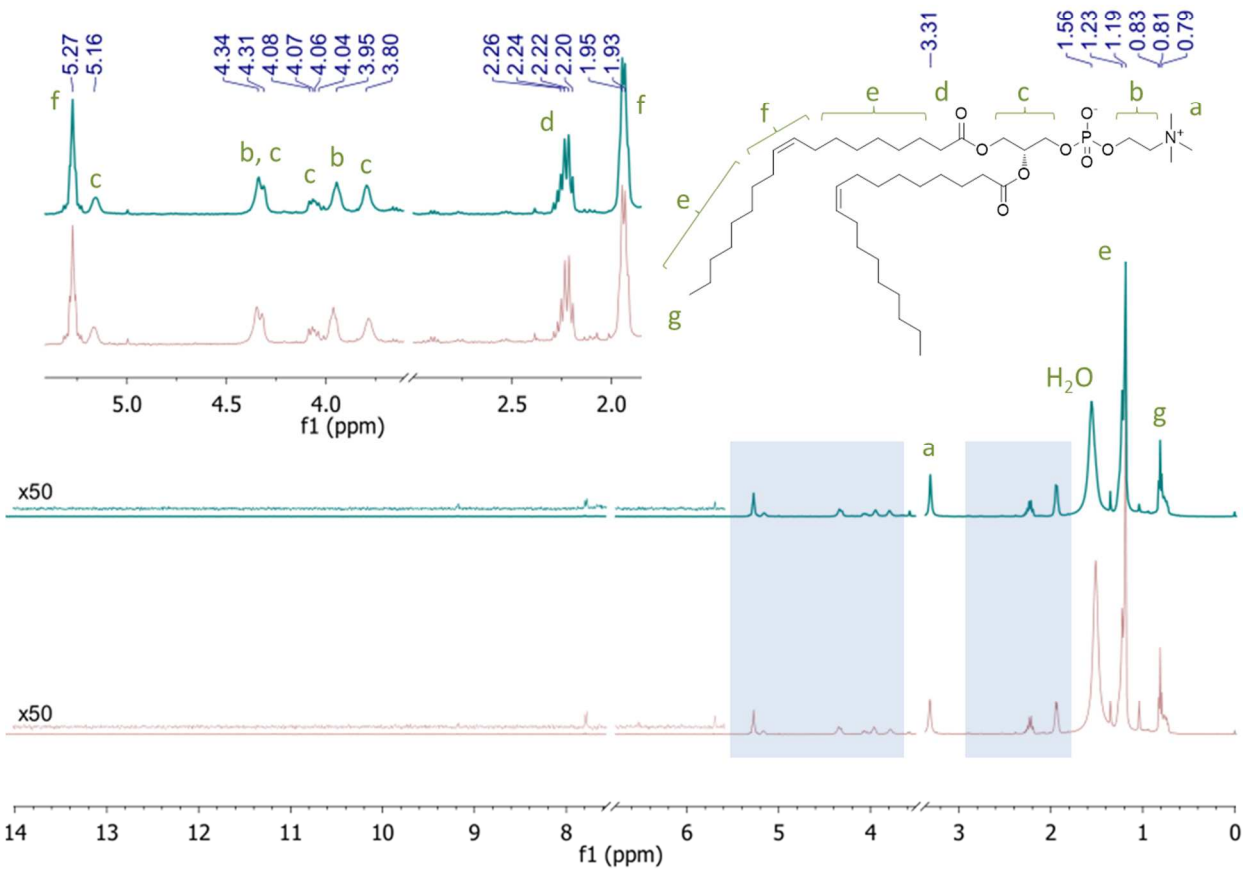

Figure 6. ^{1}H-NMR spectrum of lipids extracted from electroformed GUVs (top trace) and LMVs (bottom trace). The residual solvent peaks of chloroform (7.26 ppm) and methanol (3.49 ppm) were removed for clarity. The inset shows a magnified view of the olefinic and head group protons.

The absence of hydrolysis products was confirmed by the ^{31}P-NMR spectrum, which shows only one signal in both samples. All isomers of lyso-PC would resonate downfield, where no signal was detected.

Unilamellarity of electroformed vesicles

Vesicle unilamellarity was tested using a fluorescence quenching assay based on the measurement of the ratio of inner and outer layers of fluorescently labelled GUVs.[49,50] DOPC vesicles symmetrically labelled with the fluorescent lipid N-(7-nitrobenz-2-oxa-1,3-diazol-4-yl)-1,2-dihexadecanoyl-*sn*-glycero-3-phosphoethanolamine triethylammonium salt (NBD-PE) were electroformed and a time course of their fluorescence was measured in a plate reader. Sodium dithionite, a membrane impermeable quencher, was added to the sample in order to quench the fluorophores on the outer layer of the vesicles. The vesicles were then lysed by addition of Triton X-100, in order to expose all lipids to the quencher. The ratio between the emission drop $I_{interior}$ caused by the addition of detergent and the total emission drop $I_{total} = I_{interior} + I_{exterior}$ is used as a measure of the fraction of leaflets that are not exposed to the solvent (unilamellarity index). We measured a ratio of 51% ± 2.8%, which is consistent with unilamellarity. The measurements for all three samples are provided in the Supporting Information.

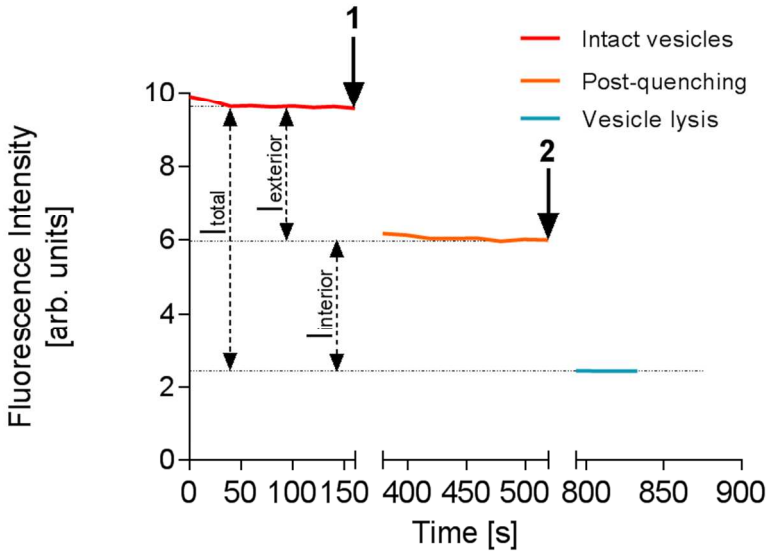

Figure 7. Fluorescence intensity measurements of DOPC:NBD-PE vesicles. The fluorescence of intact vesicles is represented from time=0 to arrow 1. At arrow 1, the quencher is added to the

suspension and the intensity is recorded until a stable value is reached. The emission drop is a measure of the number of fluorophores in outer leaflets only. At arrow 2, Triton X-100 is added to lyse the vesicles and fluorescence is recorded until a new stable value is reached. The corresponding emission drop is a measure of the number of fluorophores in inner leaflets. After each addition the plate was removed from the plate reader and shaken for several minutes (the time axis is correspondingly cut for clarity).

CONCLUSIONS

In summary, in this paper, giant vesicle electroformation using an alternative electrode material been proposed and validated. We demonstrate that electro-swelling of unilamellar vesicles occurs efficiently on stainless steel electrodes without any significant difference in vesicle size distribution, lipid degradation or leaching of metals in the electroformation chamber when compared to platinum electrodes. By using readily available stainless steel electrodes, we show that rapid, low-cost, and scalable electroformation can be achieved. We believe this platform will find application in biophysical investigations of the membrane, particularly in studies where multiplexing is crucial, such as large-scale screening of bioactive compounds.

MATERIALS AND METHODS

Electroformation chamber

The electroformation chamber (Figure 2a) is composed of two parts: the electroformation base and the chamber lid. The electroformation base (150 mm x 40 mm x 50 mm) was designed to accommodate five equidistant electroformation chambers with a length of 50 mm and diameter of 10 mm. The extremities of the chambers were tapered to increase vesicle concentration and facilitate collection of the GUVs after production. The electroformation lid (150 mm x 40 mm x 5 mm) consists of five pairs of through-holes (⌀ 1 mm) each aligned with an electroformation chamber and that are used to host the electrodes. On the side of the lid, 3 mm brass screws were positioned in correspondence to each electroformation chamber, in order to hold the electrodes in place once fully screwed. A copper bar (165 mm x 10 mm) ensures an electrical connection between corresponding electrodes. The chamber base and the lid were held together with four 4 mm screws at each corner of the device. The materials' cost of the electroformation device with five electroformation chambers was calculated to be ~£14.00. A full cost breakdown is provided in the Supporting Information.

A similar device (Figure 2b) was designed with the aim of visualising the vesicle electro-swelling process. The device was designed to be dimensionally compatible with a microscope stage and the working distance of a 40x objective. In this device, the electroformation electrodes were placed horizontally to allow the imaging of the entire electrode surface area. A 170 μm glass slide was coupled with the bottom of the chamber with silicone gel. The electrodes were connected using two sheets of stainless steel, in order to provide a common electrical connection.

The electroformation chamber was cut from a solid piece of polyoxymethylene purchased from RS Components, UK, brass screws were also supplied by RS Components, UK, and 0.8 mm 21G

50 mm needles were purchased from Becton, Dickinson and Company, USA. 1,2-Dioleoyl-*sn*-glycero-3-phosphatidylcoline (DOPC) was sourced from Avanti Polar Lipids, Inc., USA. Cholesterol, sucrose, 2-[4-(2-hydroxyethyl)piperazin-1-yl]ethanesulfonic acid (HEPES) and bovine serum albumin (BSA) were purchased from Sigma Aldrich, USA. N-(7-Nitrobenz-2-oxa-1,3-diazol-4-yl)-1,2-dihexadecanoyl-*sn*-glycero-3-phosphoethanolamine, triethylammonium salt (NBD-PE) was purchased from ThermoFisher, UK. All reagents were used as received without further purification. The electrodes were connected to an Agilent 33220A signal generator, USA set to high impedance load. GUVs were imaged in a μ-Slide 8 well multi-well plate purchased from Ibidi GmbH, Germany. Ultra-pure water (MilliQ) from a Millipore filtration system (resistivity of >18.2 MΩ·cm) was used throughout all experiments.

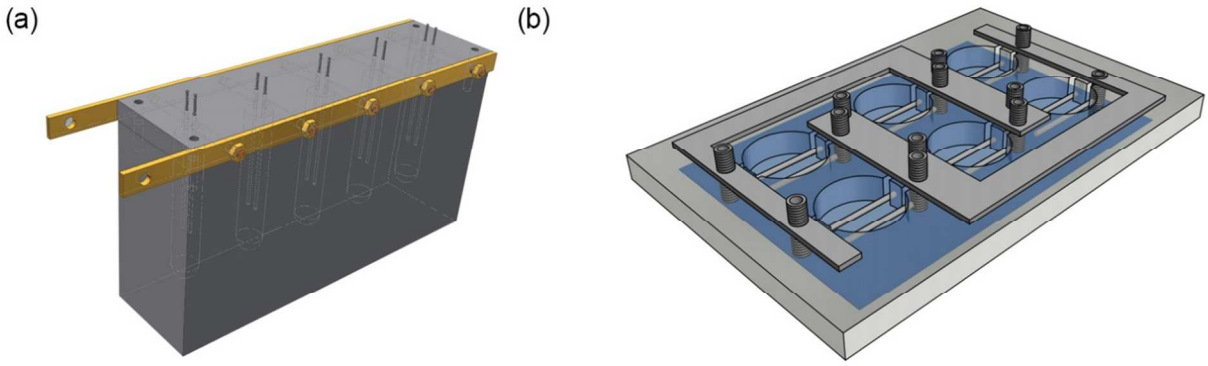

Figure 8. Vesicle electroformation devices for high-yield production and formation visualisation: (a) scalable device with five electroformation chambers and needles held by brass screws, (b) monitoring device with six chambers, brass screws and stainless steel sheets for electrical connection between common electrodes.

Electroformation protocol

The electroformation protocol consisted in preparing solutions of DOPC (1 mg/mL in chloroform) and cholesterol (10 mg/mL in chloroform) at varying molar ratios (1:0–1:3). The

electrodes were rinsed in toluene and wiped using Kimwipes (Kimberly-Clark Professional, USA) to remove any traces of silicon lubricant. The desired solution was then pipetted vertically onto the electrodes (50 µL per electrode pair) using a glass syringe, carefully coating the entire surface. After a drying phase of approximately 1 hr, the electroformation chamber was filled with sucrose solution (~3 mL, 200 mM sucrose in deionised water at room temperature), the electrodes were submerged, and the signal generator was connected via the brass screws on the sides of the chamber.

A 5 Vpp, 10 Hz sinusoidal excitation was applied for 2 hrs to induce repetitive stress on the hydrated lipid bilayer, leading to vesicle swelling. The effective voltage on the electroformation chamber was recorded using a high voltage probe and oscilloscope as 4.87 Vpp, indicating a 0.13V voltage difference due to an unmatched load of the signal generator. Subsequently, the frequency of the excitation was lowered to 5 Hz for 30 minutes to facilitate vesicle detachment. The electroformation parameters used in the protocol are summarised in Table 3. At the end of the electroformation process, the lid of the chamber was removed and the vesicles were slowly pipetted into a visualisation well using a 100-1000 µl pipette tip. To minimise the shear stress at the orifice, the end of pipette tip was cut by 2 mm using a pair of scissors. The same protocol was used for both SS304 and platinum electrodes.

Table 3. Electroformation signal generator parameters for giant unilamellar vesicle formation

Electroformation Phase	Parameters		Time (min)
	Voltage (V)	Frequency (Hz)	
I	5	10	120
II	5	5	30

GUV detection and sizing

The GUVs were imaged by phase-contrast microscopy using a Nikon ECLIPSE Ti inverted microscope (Nikon Corporation, Japan) and images were then processed using a purpose-built MATLAB® routine. The algorithm detects the GUVs based on the imfindcircles built-in MATLAB® function, calculates their diameter and plots a vesicle size histogram for all the vesicles detected.

In order to quantify the concentration of DOPC GUVs, a finite volume (100 μL) taken from the electroformation solution was placed in an 8-well imaging dish (Ibidi, UK) with 400 μL of PBS. The dish was coated with BSA by letting a 1 mg/mL BSA solution in DI water stand for two hours. The BSA solution was then rinsed gently with deionised water. After allowing the GUVs to sediment for a further two hours, the glass surface of the dish was imaged in order to cover the full area of the dish. A bounding grid that consisted of 39x45 tiles, with 10% overlap was used for stitching.

Lipid order measurements

The lateral organisation of the membrane lipids, also referred to as lipid packing, was quantified using a microscope-based spectral imaging technique.[33,51] For this purpose, an aliquot (100 μL) of GUV-rich solution was placed in an imaging well. The vesicles were then fluorescently labelled with a final concentration of 400 nM c-Laurdan, an environment-sensitive molecular probe. The solution was then diluted with 100 μL of PBS. In the case of the experiment relating lipid packing to electrode material, 400 μL of PBS was added to the solution.

The emission spectrum of c-Laurdan shifts as a function of the dipolar water relaxation, and thus the level of hydration within its surrounding microenvironment, which in turn is indicative of lipid packing in membranes. Generalised Polarisation (GP)[52] was employed as a relative measure of lipid packing on a scale of -1 to 1, where -1 represents the least packed and 1 represents the most packed membrane. Eq. 1 describes the GP relative to the intensities at two specific wavelengths: 440 (I_{440}) and 490nm (I_{490}).

$$GP = \frac{I_{440} - I_{490}}{I_{440} + I_{490}} \quad (1)$$

Spectral imaging was performed using a Zeiss LSM780 confocal microscope equipped with a 32-channel GaAsP detector array. The vesicles were excited at 405nm and the spectral intensity of the signal was recorded in the 415 to 691nm range.

Inductively coupled plasma optical emission spectrometry (ICP-OES) experiments

The concentration of metal ions in the electroformed samples was measured by ICP-OES with a Varian Vista MPX spectrometer, for both electrode materials.

Lipid extraction and NMR experiments

The samples for NMR analysis were prepared from nine simultaneous electroformation experiments. The content of each electroformation chamber (3 mL) was diluted with an equal volume of PBS in a 50 mL Falcon tube, which was then left to stand overnight at room temperature. GUV-enriched layers (500 µL each) were then withdrawn from the bottom of each Falcon tube, combined and freeze dried. The lipids were then extracted from the dried GUV samples with the Bligh and Dyer method[53]. Briefly, the sample was dispersed in water (0.8 mL), then methanol (2 mL) and chloroform (1 mL) were added with mixing after each addition. The sample was vortexed at 2500 rpm for 15 s and allowed to stand for 30 min. Chloroform (1 mL) and water (1 mL) were added, and the sample was centrifuged at 1000 g for 5 min to achieve complete phase separation. The bottom organic layer was withdrawn with a glass syringe, dried under a nitrogen stream and redissolved in $CDCl_3$ (600 µL) for analysis.

Large Multilamellar Vesicles (LMVs) control samples with different lipid concentrations were prepared using the lipid hydration method. A solution of DOPC in chloroform was added to a glass vial and dried under a nitrogen stream. The lipid film was then hydrated by adding the same sucrose solution used for electroformation and vortexed for 2 min at 2500 rpm. After adding an equal volume of PBS, the sample was left to stand at room temperature for 18 hrs. The lipids were then extracted with the same protocol used for the electroformed sample.

^{1}H-NMR spectra were acquired on a Bruker Ascend 400 spectrometer (at 400 MHz for ^{1}H and at 162 MHz for ^{31}P) with 30° pulses (Bruker zg30 sequence) and a 3s relaxation delay on a spectral width of 8000 Hz, while ^{31}P-NMR spectra were acquired with proton decoupling and a 3s relaxation delay on a spectral width of 64103 Hz. The spectra were apodised by multiplication with an exponential decay equivalent to 0.5 Hz line broadening and a Gaussian function

equivalent to 1 Hz line broadening. ^{1}H-NMR spectra were referenced to residual non deuterated chloroform, while ^{31}P-NMR spectra were externally referenced to triphenylphosphine oxide.

Vesicle unilamellarity

Three independent suspensions of fluorescently labelled vesicles were prepared using the electroformation protocol outlined previously by depositing a mixture of DOPC and NBD-PE (1 mol%) in chloroform on the electrodes. 2.7 mL of the GUV suspension were then mixed with 300 µL of a HEPES buffer at pH 7 (0.1 M HEPES and 1 M NaCl) to obtain final concentrations of 10 mM HEPES and 100 mM NaCl. Three wells of a 96 well plate were filled were filled with 200 µL of the buffered GUV suspension. Stable values of fluorescence intensity were measured at 520 nm on a FLUOstar Omega plate reader (BMG Labtech) before and after adding 4 µL of a freshly prepared solution of 1 M $Na_2S_2O_4$ in 1 M Tris buffer at pH 10, with excitation at 485 nm. Subsequently, 20 µL of a 10% v/v solution of Triton X-100 were added to the solution to cause vesicle lysis and expose all lipid structures to the quencher. A final stable value of fluorescence was recorded after the addition of the detergent. The unilamellarity index, defined as the fraction of leaflets that are not exposed to the solvent, was calculated as the ratio between the emission drop $I_{interior}$ caused by the addition of detergent and the total emission drop $I_{total} = I_{interior} + I_{exterior}$.

Statistical analyses

Statistical testing was performed using one-way ANOVA for multiple comparison analysis while a Student's t-test was employed for direct comparison between two data sets. All data are expressed in terms of mean ± standard deviation and the number of independent replicates is expressed in the figure captions. The following conventions for statistical significance are used throughout the paper: ns = $p > 0.05$, * = $p \leq 0.05$, ** = $p \leq 0.01$, *** = $p \leq 0.001$, **** = $p \leq 0.0001$.

ASSOCIATED CONTENT

Supporting Information.

The following files are available free of charge.

Information on the cost breakdown of the electroformation chamber, limit of detection in NMR experiments and data on unilamellarity experiments are provided in the file (PDF)

Video of vesicles forming on a SS304 electrode upon application of an external electric field at t=3 s (scale bar = 20 μm) (mp4)

Photograph of electroformation chamber (jpeg)

AUTHOR INFORMATION

Corresponding Author

Professor Eleanor Stride

Email: eleanor.stride@eng.ox.ac.uk

Phone: +44 (0)1865 617747

Mailing address: Institute of Biomedical Engineering, Old Road Campus Research Building, University of Oxford, Oxford OX3 7DQ, UK

Author Information

Mr. Valerio Pereno

Email: valerio.pereno@eng.ox.ac.uk

Phone: +44 (0)1865 617726

Mailing address: Institute of Biomedical Engineering, Old Road Campus Research Building, University of Oxford, Oxford OX3 7DQ, UK

Dr. Dario Carugo

Email: d.carugo@soton.ac.uk

Phone: +44 (0)2380 595769

Mailing address: Mechatronics and Bioengineering Science research groups, Faculty of Engineering and the Environment, University of Southampton, SO17 1BJ, Southampton, United Kingdom

Dr. Luca Bau

Email: luca.bau@eng.ox.ac.uk

Phone: +44 (0)1865 617726

Mailing address: Mailing address: Institute of Biomedical Engineering, Old Road Campus Research Building, University of Oxford, Oxford OX3 7DQ, UK

Dr. Erdinc Sezgin

Email: erdinc.sezgin@rdm.ox.ac.uk

Phone: +44 (0)1865 222484

Mailing address: Wetherall Institute of Molecular Medicine, Department of Immunology, University of Oxford, Oxford, OX3 9DS, United Kingdom

Dr. Jorge Bernardino de la Serna

Email: jorge.bernardino-de-la-serna@stfc.ac.uk

Phone: +44 (0) 01235 445460

Mailing address: Science and Technology Facilities Council, Rutherford Appleton Laboratory, Central Laser Facility, Research Complex at Harwell, Harwell-Oxford, OX11 0FA, United Kingdom

Professor Christian Eggeling

Email: christian.eggeling@rdm.ox.ac.uk

Phone: +44 (0)1865 222167

Mailing address: Wetherall Institute of Molecular Medicine, Department of Immunology, University of Oxford, Oxford, OX3 9DS, United Kingdom

Author Contributions

The manuscript was written through contributions of all authors. All authors have given approval to the final version of the manuscript.

Funding Sources

This work was supported by EPSRC Grant EP/I021795/1. E. Sezgin and C. Eggeling thank Wolfson Foundation, the Medical Research Council (MRC, grant number MC_UU_12010/unit programmes G0902418 and MC_UU_12025), MRC/BBSRC/ESPRC (grant number MR/K01577X/1), and the Wellcome Trust (grant ref 104924/14/Z/14). E. Sezgin is supported by EMBO Long Term and Marie Curie Intra-European Fellowships (MEMBRANE DYNAMICS). J. Bernardino de la Serna acknowledges support from the Marie Curie Career Integration Grant.

ACKNOWLEDGMENT

We would like to extend our gratitude to James Fisk and David Salisbury for the fabrication of the electroformation chambers, Graham Brown for helpful discussions on microscopy techniques, and Fabio Bianchi for the helpful technical discussions.

ABBREVIATIONS

GUV, giant unilamellar vesicle; LMV large multilamellar vesicle; E, electric field; DOPC, 1,2-dioleoyl-sn-glycero-3-phosphatidylcholine; 1,2-distearoyl-sn-glycero-3-phosphocholine, DSPC; 1,2-dipalmitoyl-sn-glycero-3-phosphocholine, DPPC; 1,2-dimyristoyl-sn-glycero-3-phosphocholine, DMPC; indium tin oxide, ITO; nuclear magnetic resonance, NMR; proton nuclear magnetic resonance, H-NMR; inductively coupled plasma optical emission spectrometry, ICP-OES, phosphate-buffered saline, PBS; peak-to-peak voltage, Vpp;

REFERENCES

(1) Lingwood, D.; Simons, K. Lipid Rafts as a Membrane-Organizing Principle. *Science* **2010**, *327*, 46–50.

(2) Bagatolli, L. a; Gratton, E. A Correlation between Lipid Domain Shape and Binary Phospholipid Mixture Composition in Free Standing Bilayers : A Two-Photon Fluorescence Microscopy Study. *Biophys. J.* **2000**, *79*, 434–447.

(3) Dietrich, C.; Bagatolli, L. a; Volovyk, Z. N.; Thompson, N. L.; Levi, M.; Jacobson, K.; Gratton, E. Lipid Rafts Reconstituted in Model Membranes. *Biophys. J.* **2001**, *80*, 1417–1428.

(4) Korlach, J.; Schwille, P.; Webb, W. W.; Feigenson, G. W. Characterization of Lipid Bilayer Phases by Confocal Microscopy and Fluorescence Correlation Spectroscopy. *Proc. Natl. Acad. Sci. U. S. A.* **1999**, *96*, 8461–8466.

(5) Feigenson, G. W.; Buboltz, J. T. Ternary Phase Diagram of Dipalmitoyl-PC/Dilauroyl-PC/Cholesterol: Nanoscopic Domain Formation Driven by Cholesterol. *Biophys. J.* **2001**, *80*, 2775–2788.

(6) Veatch, S. L.; Keller, S. L. Separation of Liquid Phases in Giant Vesicles of Ternary Mixtures of Phospholipids and Cholesterol. *Biophys. J.* **2003**, *85*, 3074–3083.

(7) Sun, T. L.; Sun, Y.; Lee, C. C.; Huang, H. W. Membrane Permeability of Hydrocarbon-Cross-Linked Peptides. *Biophys. J.* **2013**, *104*, 1923–1932.

(8) Nishimura, K.; Matsuura, T.; Sunami, T.; Fujii, S.; Nishimura, K.; Suzuki, H.; Yomo, T.

Identification of Giant Unilamellar Vesicles with Permeability to Small Charged Molecules. *RSC Adv.* **2014**, *4*, 35224.

(9) Staykova, M.; Lipowsky, R.; Dimova, R. Membrane Flow Patterns in Multicomponent Giant Vesicles Induced by Alternating Electric Fields. *Soft Matter* **2008**, *4*, 2168.

(10) Fenz, S. F.; Sengupta, K. Giant Vesicles as Cell Models. *Integr. Biol.* **2012**, *4*, 982.

(11) Nappini, S.; Kayal, A.; Berti, D.; Nord En, B.; Baglioni, P. Magnetically Triggered Release From Giant Unilamellar Vesicles: Visualization By Means Of Confocal Microscopy. *J. Phys. Chem. Lett* **2011**, *2*, 713–718.

(12) Dubavik, A.; Sezgin, E.; Lesnyak, V.; Gaponik, N.; Schwille, P.; Eychm??ller, A. Penetration of Amphiphilic Quantum Dots through Model and Cellular Plasma Membranes. *ACS Nano* **2012**, *6*, 2150–2156.

(13) Bernardino de la Serna, J.; Perez-Gil, J.; Simonsen, A. C.; Bagatolli, L. A. Cholesterol Rules. *J. Biol. Chem.* **2004**, *279*, 40715–40722.

(14) Bernardino de la Serna, J.; Hansen, S.; Berzina, Z.; Simonsen, A. C.; Hannibal-Bach, H. K.; Knudsen, J.; Ejsing, C. S.; Bagatolli, L. A. Compositional and Structural Characterization of Monolayers and Bilayers Composed of Native Pulmonary Surfactant from Wild Type Mice. *Biochim. Biophys. Acta - Biomembr.* **2013**, *1828*, 2450–2459.

(15) Heinrich, M. C.; Capraro, B. R.; Tian, A.; Isas, J. M.; Langen, R.; Baumgart, T. Quantifying Membrane Curvature Generation of Drosophila Amphiphysin N-BAR Domains. *J. Phys. Chem. Lett* **2010**, *1*, 3401–3406.

(16) López-Montero, I.; Rodríguez-García, R.; Monroy, F. Artificial Spectrin Shells

Reconstituted on Giant Vesicles. *J. Phys. Chem. Lett.* **2012**, *3*, 1583–1588.

(17) Caschera, F.; Serna, J. B. de la; Löffler, P. M. G.; Rasmussen, T. E.; Hanczyc, M. M.; Bagatolli, L. A.; Monnard, P.-A. Stable Vesicles Composed of Monocarboxylic or Dicarboxylic Fatty Acids and Trimethylammonium Amphiphiles. **2011**.

(18) Walde, P.; Cosentino, K.; Engel, H.; Stano, P. Giant Vesicles: Preparations and Applications. *ChemBioChem* **2010**, *11*, 848–865.

(19) Méléard, P.; Bagatolli, L. A.; Pott, T. Giant Unilamellar Vesicle Electroformation: From Lipid Mixtures to Native Membranes under Physiological Conditions. *Methods Enzymol.* **2009**, *465*, 161–176.

(20) Dimova, R.; Aranda, S.; Bezlyepkina, N.; Nikolov, V.; Riske, K. a; Lipowsky, R. A Practical Guide to Giant Vesicles. Probing the Membrane Nanoregime via Optical Microscopy. *J. Phys. Condens. Matter* **2006**, *18*, S1151-76.

(21) Reeves, J. P.; Dowben, R. M. Formation and Properties of Thin-Walled Phospholipid Vesicles. *J. Cell. Physiol.* **1969**, *73*, 49–60.

(22) Angelova, M. I.; Dimitrov, D. S. Liposome Electroformation. *Faraday Discuss. Chem. Soc.* **1986**, *81*, 303.

(23) Pautot, S.; Frisken, B. J.; Weitz, D. a. Production of Unilamellar Vesicles Using an Inverted Emulsion. *Langmuir* **2003**, *19*, 2870–2879.

(24) Yamada, A.; Le Berre, M.; Yoshikawa, K.; Baigl, D. Spontaneous Generation of Giant Liposomes from an Oil/water Interface. *ChemBioChem* **2007**, *8*, 2215–2218.

(25) Stachowiak, J. C.; Richmond, D. L.; Li, T. H.; Liu, A. P.; Parekh, S. H.; Fletcher, D. a. Unilamellar Vesicle Formation and Encapsulation by Microfluidic Jetting. *Proc. Natl. Acad. Sci. U. S. A.* **2008**, *105*, 4697–4702.

(26) Arriaga, L. R.; Datta, S. S.; Kim, S. H.; Amstad, E.; Kodger, T. E.; Monroy, F.; Weitz, D. a. Ultrathin Shell Double Emulsion Templated Giant Unilamellar Lipid Vesicles with Controlled Microdomain Formation. *Small* **2014**, *10*, 950–956.

(27) Bi, H.; Yang, B.; Wang, L.; Cao, W.; Han, X. Electroformation of Giant Unilamellar Vesicles Using Interdigitated ITO Electrodes. *J. Mater. Chem. A* **2013**, *1*, 7125.

(28) Aimon, S.; Manzi, J.; Schmidt, D.; Poveda Larrosa, J. A.; Bassereau, P.; Toombes, G. E. S. Functional Reconstitution of a Voltage-Gated Potassium Channel in Giant Unilamellar Vesicles. *PLoS One* **2011**, *6*, e25529.

(29) Fidorra, M.; Duelund, L.; Leidy, C.; Simonsen, A. C.; Bagatolli, L. A. Absence of Fluid-Ordered/Fluid-Disordered Phase Coexistence in Ceramide/POPC Mixtures Containing Cholesterol. *Biophys. J.* **2006**, *90*, 4437–4451.

(30) Montes, L.; Alonso, A.; Goni, F. M.; Bagatolli, L. A. Giant Unilamellar Vesicles Electroformed from Native Membranes and Organic Lipid Mixtures under Physiological Conditions. *Biophys. J.* **2007**, *93*, 3548–3554.

(31) Lecuyer, S.; Ristenpart, W. D.; Vincent, O.; Stone, H. a. Electrohydrodynamic Size Stratification and Flow Separation of Giant Vesicles. *Appl. Phys. Lett.* **2008**, *92*.

(32) Herold, C.; Chwastek, G.; Schwille, P.; Petrov, E. P. Efficient Electroformation of Supergiant Unilamellar Vesicles Containing Cationic Lipids on ITO-Coated Electrodes.

Langmuir **2012**, *28*, 5518–5521.

(33) Sezgin, E.; Sadowski, T.; Simons, K. Measuring Lipid Packing of Model and Cellular Membranes with Environment Sensitive Probes. *Langmuir* **2014**, *30*, 8160–8166.

(34) Silvius, J. R. Role of Cholesterol in Lipid Raft Formation: Lessons from Lipid Model Systems. *Biochim. Biophys. Acta - Biomembr.* **2003**, *1610*, 174–183.

(35) Veatch, S. L.; Keller, S. L. Organization in Lipid Membranes Containing Cholesterol. *Phys. Rev. Lett.* **2002**, *89*, 268101.

(36) Söderlund, T.; Alakoskela, J.-M. I.; Pakkanen, A. L.; Kinnunen, P. K. J. Comparison of the Effects of Surface Tension and Osmotic Pressure on the Interfacial Hydration of a Fluid Phospholipid Bilayer. *Biophys. J.* **2003**, *85*, 2333–2341.

(37) Lis, L. J.; Lis, W. T.; Parsegian, V. a; Rand, R. P. Adsorption of Divalent Cations to a Variety of Phosphatidylcholine Bilayers. *Biochemistry* **1981**, *20*, 1771–1777.

(38) Suwalsky, M.; Castro, R.; Villena, F.; Sotomayor, C. P. Cr(III) Exerts Stronger Structural Effects than Cr(VI) on the Human Erythrocyte Membrane and Molecular Models. *J. Inorg. Biochem.* **2008**, *102*, 842–849.

(39) Binder, H.; Zschörnig, O. The Effect of Metal Cations on the Phase Behavior and Hydration Characteristics of Phospholipid Membranes. *Chem. Phys. Lipids* **2002**, *115*, 39–61.

(40) Ohki, S.; Düzgünes, N. Divalent Cation-Induced Interaction of Phospholipid Vesicle and Monolayer Membranes. *BBA - Biomembr.* **1979**, *552*, 438–449.

(41) Stohs, S. J.; Bagchi, D. Oxidative Mechanisms in the Toxicity of Metal Ions. *Free Radic. Biol. Med.* **1995**, *18*, 321–336.

(42) Ayuyan, A. G.; Cohen, F. S. Lipid Peroxides Promote Large Rafts: Effects of Excitation of Probes in Fluorescence Microscopy and Electrochemical Reactions during Vesicle Formation. *Biophys. J.* **2006**, *91*, 2172–2183.

(43) Mills, J. K.; Needham, D. Lysolipid Incorporation in Dipalmitoylphosphatidylcholine Bilayer Membranes Enhances the Ion Permeability and Drug Release Rates at the Membrane Phase Transition. *Biochim. Biophys. Acta - Biomembr.* **2005**, *1716*, 77–96.

(44) Fuller, N.; Rand, R. P. The Influence of Lysolipids on the Spontaneous Curvature and Bending Elasticity of Phospholipid Membranes. *Biophys. J.* **2001**, *81*, 243–254.

(45) Sparling, M. L.; Zidovetzki, R.; Muller, L.; Chan, S. I. Analysis of Membrane Lipids by 500 MHz 1H NMR. *Anal. Biochem.* **1989**, *178*, 67–76.

(46) Nieva-Echevarr??a, B.; Goicoechea, E.; Manzanos, M. J.; Guill??n, M. D. Usefulness of 1H NMR in Assessing the Extent of Lipid Digestion. *Food Chem.* **2015**, *179*, 182–190.

(47) Kriat, M.; Vion-Dury, J.; Confort-Gouny, S.; Favre, R.; Viout, P.; Sciaky, M.; Sari, H.; Cozzone, P. J. Analysis of Plasma Lipids by NMR Spectroscopy: Application to Modifications Induced by Malignant Tumors. *J. Lipid Res.* **1993**, *34*, 1009–1019.

(48) MacKenzie, A.; Vyssotski, M.; Nekrasov, E. Quantitative Analysis of Dairy Phospholipids by 31P NMR. *J. Am. Oil Chem. Soc.* **2009**, *86*, 757–763.

(49) McIntyre, J. C.; Sleight, R. G. Fluorescence Assay for Phospholipid Membrane Asymmetry. *Biochemistry* **1991**, *30*, 11819–11827.

(50) Gruber, H. J.; Schindler, H. External Surface and Lamellarity of Lipid Vesicles: A Practice-Oriented Set of Assay Methods. *Biochim. Biophys. Acta - Biomembr.* **1994**, *1189*, 212–224.

(51) Sezgin, E.; Waithe, D.; Bernardino de la Serna, J.; Eggeling, C. Spectral Imaging to Measure Heterogeneity in Membrane Lipid Packing. *Chemphyschem* **2015**, *16*, 1387–1394.

(52) Parasassi, T.; De Stasio, G.; Ravagnan, G.; Rusch, R. M.; Gratton, E. Quantitation of Lipid Phases in Phospholipid Vesicles by the Generalized Polarization of Laurdan Fluorescence. *Biophys. J.* **1991**, *60*, 179–189.

(53) E. G. Bligh; W. J. Dyer. A Rapid Method of Total Lipid Extraction and Purification. *Can. J. Biochem. Physiol.* **1959**, *37*.

TOC GRAPHICS